Disruption of the plasma membrane stimulates rearrangement of microtubules and lipid traffic toward the wound site

Tatsuru Togo

Misaki Marine Biological Station, University of Tokyo, 1024 Ko-Ajiro, Misaki, Miura, Kanagawa 238-0225, Japan
e-mail: togot@mmbs.s.u-tokyo.ac.jp

Accepted 4 April 2006
Journal of Cell Science 119, 2780-2786 Published by The Company of Biologists 2006
doi:10.1242/jcs.03006

Summary

Resealing of a disrupted plasma membrane requires Ca^{2+}-regulated exocytosis. Repeated disruptions reseal more quickly than the initial wound. This facilitated response requires both Ca^{2+} and protein kinase C (PKC), and is sensitive to brefeldin A. There is also evidence that this response is polarized to the site where the cell membrane had previously been disrupted. Observations of GFP-tagged α-tubulin and end-binding protein 1 (EB1) revealed that membrane disruption initially induced disassembly of microtubules around the wound site, followed by elongation of microtubules toward the wound site. Recruitment of EB1 to microtubules required Ca^{2+} influx, but was independent of PKC. NBD C_6-ceramide, a probe for the Golgi apparatus and Golgi-derived lipids, initially stained the perinuclear region, and a portion of the probe was translocated to the wound site 5 minutes after wounding. Translocation of the lipids required microtubules and PKC activity, and was suppressed by low temperature. On the other hand, constitutive traffic of the lipid was still normal in the presence of a PKC inhibitor. These findings suggest that membrane disruption stimulates regulated vesicle traffic from the region of the trans-Golgi network to the wound site along rearranged microtubules in a PKC-dependent manner.

Supplementary material available online at
http://jcs.biologists.org/cgi/content/full/119/13/2780/DC1

Key words: Membrane resealing, Microtubule, EB1, NBD C_6-ceramide

Introduction

Plasma membrane disruptions are widespread and normal events in many animal tissues. Cell survival following plasma membrane disruption depends on rapid resealing of the cell membrane. The energy-dependent processes involved in plasma membrane resealing are triggered by Ca^{2+} influx through the wound (McNeil and Steinhardt, 2003). Plasma membrane resealing by lipid bilayer reorganization requires a reduction in cell membrane tension that is mediated by Ca^{2+}-regulated exocytosis of internal vesicles (Togo et al., 2000).

When cells are wounded twice, the second membrane disruption generally reseals more quickly than the initial wound (Togo et al., 1999; Togo et al., 2003). The faster membrane resealing is due to an increased amount of exocytosis after repeated wounds. Two different signaling responses, potentiated and facilitated, have been described, dependent on the site of the second wound relative to the first (Togo et al., 2003). The potentiated response is characterized by a faster resealing response to a second wound at a different site. On the other hand, the facilitated response is characterized by a faster resealing response to a second wound at the same initial wound site, depends on both a threshold extracellular Ca^{2+} concentration and protein kinase C (PKC) activity, and is sensitive to brefeldin A (BFA) (Togo et al., 1999; Togo et al., 2003; Shen and Steinhardt, 2005). Specifically, when the same site of a cell membrane is wounded twice within 5 minutes in the presence of Gö-6976, a specific inhibitor for PKC-α and β_1 (Martiny-Baron et al., 1993), facilitation of membrane resealing at a second wound is inhibited (Togo et al., 1999; Togo et al., 2003). However, inhibition of PKC by Gö-6976 has no effect on the facilitation of second wound resealing at a different wound site (Togo et al., 2003). BFA inhibition of vesicle traffic from the Golgi complex (Klausner et al., 1992) produces a similar pattern of inhibition of facilitation for second wounds at the same or different sites as does Gö-6976 (Togo et al., 1999; Togo et al., 2003; Shen and Steinhardt, 2005). BFA does not affect membrane resealing after an initial wound (Togo et al., 1999), even though several studies have shown that BFA also induces membrane tubulation of endosomes and lysosomes (Klausner et al., 1992). These results strongly suggest that membrane traffic from the region of the trans-Golgi network (TGN) is directed toward the site where the vesicle pool has been depleted by a previous membrane disruption.

One aim of the present study was to clarify the behavior of microtubules (MTs) upon cell membrane disruption, because the long-range transport from the Golgi/TGN occurs along MTs (Toomre et al., 1999; Schmoranzer and Simon, 2003; Schmoranzer et al., 2003). To monitor the behavior of MTs, green fluorescent protein (GFP)-tagged α-tubulin and end-binding protein 1 (EB1), a MT plus-end-tracking protein, were expressed in PtK2 cells. This study provides the first evidence that Ca^{2+} influx upon cell membrane disruption regulates the subcellular recruitment of EB1 to the MTs, resulting in the

rearrangement of MTs. Furthermore, by use of a fluorescent lipid probe, this work also shows that regulated vesicle traffic toward the plasma membrane from the region of the TGN is stimulated by membrane disruption.

Results

Cell membrane disruption induces disassembly and reassembly of MTs around the wound site

To monitor the behavior of MTs, a vector encoding EGFP-α-tubulin was transfected into PtK2 cells. Cells expressing EGFP-α-tubulin were wounded with a glass needle and were observed by conventional inverted fluorescent microscopy. Since PtK2 cells are extremely flat, the behavior of MTs can be adequately monitored in a single focal plane (Toomre et al., 1999). When cells were wounded in 1.8 mM Ca^{2+} Ringer's solution, cell membrane disruption initially induced disassembly of MTs around the wound site (Fig. 1A). The disassembled area propagated from the wound site for 16.25±1.25 seconds at the rate of 0.923±0.071 μm/second (5 cells). Within 30 seconds of membrane disruption, initiation of MT reassembly could be detected. A typical time-lapse sequence is shown in Fig. 1B. Measurements of the distance between MT ends and the wound site revealed that MTs spent most of the time approaching (73.2%); as a result, MT ends continuously approached the wound site (Fig. 1C). The average approach rate was 2.14±0.17 μm/minute. Similar reassembly of MTs was observed in four out of four cells.

EB1 is a member of a conserved protein family that localizes to polymerizing MT plus ends and can promote MT assembly (Tirnauer and Bierer, 2000; Schuyler and Pellman, 2001; Tirnauer et al., 2002; Busch and Brunner, 2004). To detect growing MT plus ends, EB1-GFP was expressed in PtK2 cells. Fluorescent 'comets' with bright fronts and dimmer 'tails' were observed at the elongating MTs in PtK2 cells, as described in other cells (Mimori-Kiyosue et al., 2000; Ma et al., 2004; Salaycik et al., 2005). There were also faint MT images in addition to the comets. These MT images disappeared during recording possibly as a result of photobleaching. When the cell was wounded in 1.8 mM Ca^{2+} Ringer's solution, numerous comets appeared around the wound site within 30 seconds of cell membrane disruption (arrowheads in Fig. 2A), and some comets approached the wound site (arrows in Fig. 2A) (see also supplementary material, Movie 1). A small increase in brighter EB1 comets was also observed throughout the cell, but the obvious increase in the number of comets observed around the wound site was not observed throughout the cell (Fig. 2B and supplementary material, Movie 2). The same results were obtained in all five cells examined. These experiments clearly indicate that membrane disruption induces both recruitment of EB1 to the disassembled MTs and elongation of MT ends especially around the wound site.

Reassembly of MTs upon cell membrane disruption is Ca^{2+}-dependent, but not PKC-dependent

To investigate the involvement of Ca^{2+} in MT dynamics, Ca^{2+} concentration was lowered from 1.8 mM to 0.4 mM. 0.4 mM Ca^{2+} is well above the threshold level required for membrane resealing although the rate of the resealing is slowed (Steinhardt et al., 1994; Bi et al., 1995). Therefore cells can usually survive both initial and second wounds, but the facilitated response at the second membrane resealing is suppressed (Togo et al., 1999). When cells expressing EGFP-α-tubulin were wounded in 0.4 mM Ca^{2+} Ringer's solution, disassembly of MTs around the wound site was induced (Fig. 3A). Propagation of the MT disassembled area continued for 46.00±1.87 seconds (six cells), which was about 2.8 times longer than in 1.8 mM Ca^{2+} Ringer's solution, and the rate was about four times slower than in 1.8 mM Ca^{2+} Ringer's solution (0.228±0.008 μm/second, six cells). These results indicate that Ca^{2+} influx through the wound site promotes MT disassembly.

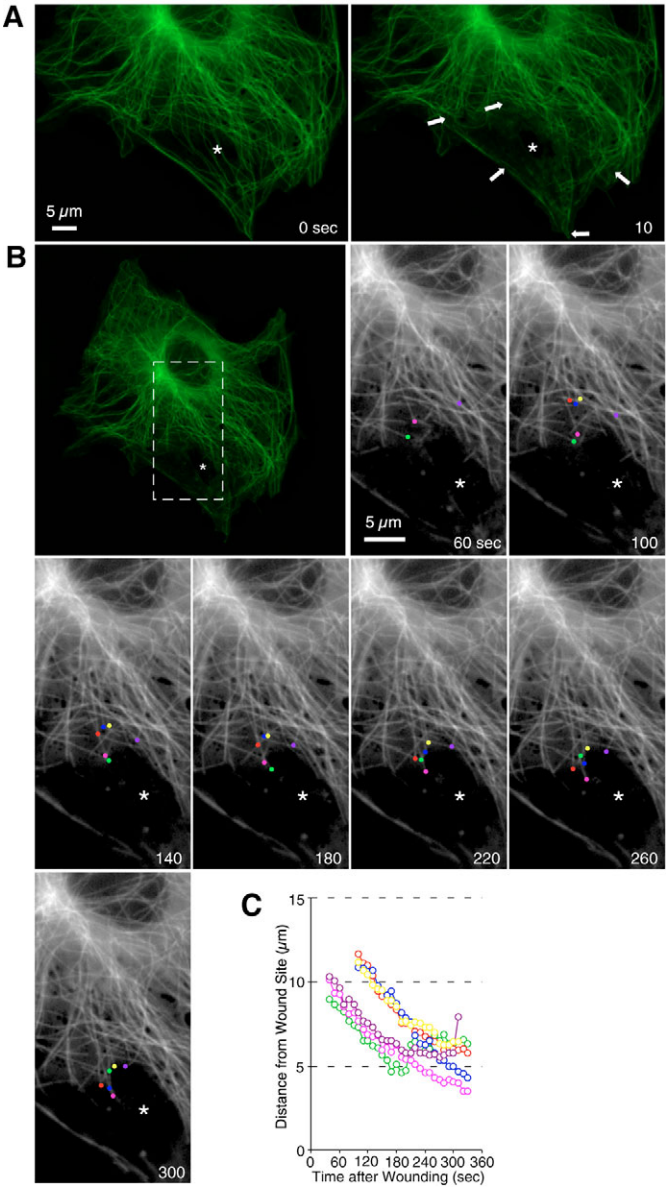

Fig. 1. Disruption of the cell membrane induces disassembly and reassembly of MTs. (A) A PtK2 cell expressing α-tubulin-EGFP was wounded by a glass needle in 1.8 mM Ca^{2+} Ringer's solution. The asterisk indicates the site of cell membrane disruption. The membrane disruption initially induced MT disassembly around the wound site. Arrows indicate examples of disassembled MTs. (B,C) Plus-end tips of disassembled MTs approached the wound site in 1.8 mM Ca^{2+} Ringer's solution. Colored dots indicate selected MT ends.

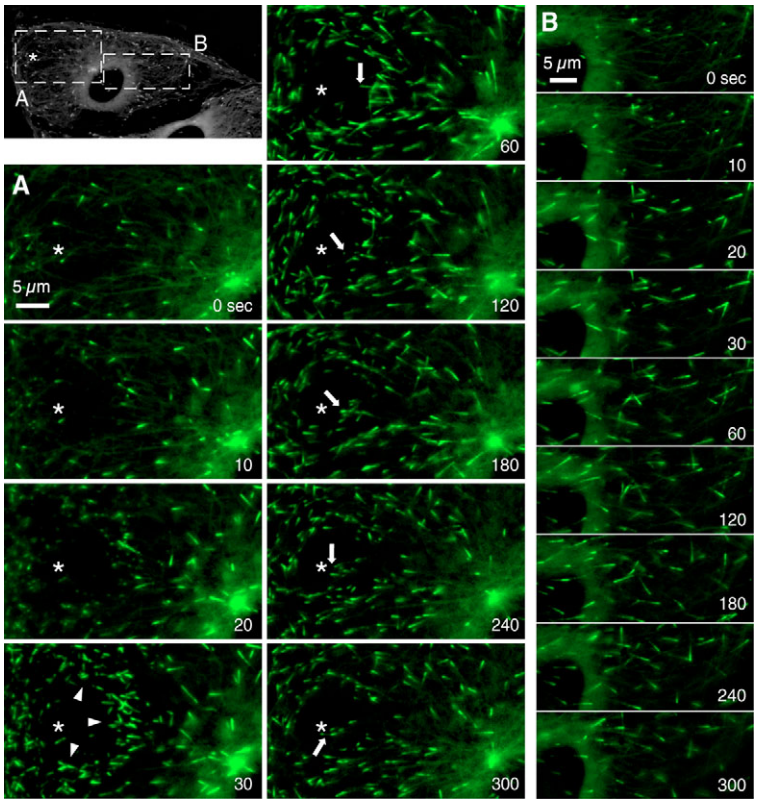

Fig. 2. Visualization of EB1-GFP reveals the approach of MT plus-end tips toward the wound site. A PtK2 cell expressing EB1-GFP was wounded in 1.8 mM Ca^{2+} Ringer's solution. The asterisk indicates the site of the cell membrane disruption. A slight increase in the number of bright EB1-GFP 'comets' was observed throughout the cell. Furthermore, numerous EB1 comets appeared around the wound site within 30 seconds of membrane disruption (arrowheads). Some comets approached the wound site (arrows). Movies are available in supplementary material (Movies 1 and 2).

It has already been shown that Ca^{2+} stimulates MT disassembly by specifically promoting the catastrophe reaction (O'Brien et al., 1997).

Sustained movement of plus-end tips of disassembled MTs toward the wound site could not be detected in 0.4 mM Ca^{2+} Ringer's solution. A typical time-lapse sequence is shown in Fig. 3B. For instance, an MT end indicated by a green dot in Fig. 3B approached the wound site 60-140 seconds after membrane disruption, but left the wound site after that. There were also MTs that did not approach the wound site at all during observation. Measurements of the distance between the wound site and the MT ends also indicated that behavior of MTs was independent of the wound site (Fig. 3C). These observations were reproduced five times in independent experiments.

When cells expressing EB1-GFP were wounded in 0.4 mM Ca^{2+} Ringer's solution, a slight increase in the bright EB1 comets was observed throughout the cell (Fig. 4B). However, there was no obvious directional movement of EB1 comets toward the wound site (Fig. 4A and supplementary material, Movie 3). Similar results were obtained from five other cells. These observations indicate that EB1 recruitment to the MTs around the wound site is induced by massive Ca^{2+} influx through the wound site.

The facilitated response of membrane resealing is suppressed by a specific PKC inhibitor, Gö-6976 (Togo et al., 1999). To examine the effect of PKC inhibition on the behavior of MTs, cells expressing EGFP-α-tubulin were wounded in 1.8 mM Ca^{2+} Ringer's solution containing 1 μM Gö-6976. Disassembly of MTs upon cell membrane disruption was induced as in control experiments. The disassembled area propagated from the wound site for 15.00±1.09 seconds at the rate of 0.958±0.167 μm/second (five cells). Within 30 seconds of membrane disruption, approach of MT plus-end tips toward the wound site could be detected in five out of six cells. As in the control experiment, disassembled MTs spent more time approaching (84.4%), resulting in continuous elongation toward the wound site. The average approach rate was 2.73±0.65 μm/minute.

To observe growing MT plus ends, cells expressing EB1-GFP were wounded in the presence of 1 μM Gö-6976 in 1.8 mM Ca^{2+} Ringer's solution. A typical time-lapse sequence is shown in Fig. 5. Within 30 seconds of cell membrane disruption, numerous EB1-GFP comets appeared around the wound site (arrowheads in Fig. 5A), and some comets approached the wound site (arrows in Fig. 5A), as observed in control experiments (see also supplementary material, Movie 4). There was also an increase in the number of brighter EB1 comets throughout the cell as observed in the control experiments (Fig. 5B). These results indicate that rearrangement of MTs upon cell membrane disruption is not sensitive to Gö-6976, and suggest that PKCs that are inhibited by Gö-6976 may have other targets than the MTs during facilitated response.

Cell membrane disruption stimulates delivery of NBD lipids toward the wound site

NBD C_6-ceramide is a vital stain for the Golgi complex, and has been used as a tool for studying lipid traffic between the Golgi and the plasma membrane (Lipsky and Pagano, 1985a; Lipsky and Pagano, 1985b). NBD C_6-ceramide is metabolized in living cells to sphingomyelin and a glucosylceramide, and these fluorescent metabolites are subsequently transported to the cell membrane from the Golgi complex by a vesicle-mediated process (Lipsky and Pagano, 1985b). To monitor the translocation of NBD C_6-ceramide and its metabolites upon cell membrane disruption, PtK2 cells were loaded with 5 μM NBD C_6-ceramide as described in the Materials and Methods. As reported previously (Lipsky and Pagano, 1985b), the probe initially stained the Golgi, and 2 hours later the entire surface of the cell became fluorescent in addition to the Golgi, if cells were not wounded (data not shown). When cells were wounded in 1.8 mM Ca^{2+} Ringer's solution, the region around the wound site was visibly fluorescent 5 minutes after the wounding (Fig. 6A).

When cells were treated with 1 μM Gö-6976 in 1.8 mM-Ca^{2+} Ringer's solution, fluorescent lipids were not observed around the wound site (Fig. 6B). When the cell was incubated in 1 μM Gö-6976 without wounding, the entire surface of the cell became fluorescent 2 hours later, as observed in a control experiment. These results indicate that constitutive traffic of

fluorescent lipids is not sensitive to Gö-6976, but regulated traffic upon cell membrane disruption is sensitive to Gö-6976.

To examine the effect of MT disassembly on the appearance of the fluorescent spot around the wound site, cells were loaded with NBD C_6-ceramide in the presence of 1 μg/ml nocodazole, and further incubated with 1 μg/ml nocodazole for 30 minutes at 37°C before wounding. As shown in Fig. 6C, appearance of a fluorescent spot around the wound site was inhibited by treatment with nocodazole, indicating that lipid traffic toward the wound site required MTs.

It has been known that incubation at low temperature blocks vesicle transport from the Golgi complex (Matlin and Simons, 1983; Saraste and Kuismanen, 1984). As shown previously, incubation at low temperature (20°C) does not inhibit membrane resealing at the initial wound, but the facilitated response of second membrane resealing is specifically suppressed (Togo et al., 1999). When cells were wounded at 20°C, fluorescent lipids could not be detected around the wound site (Fig. 6D).

To determine the effect of nocodazole on membrane resealing, cells were loaded with 1 μM calcein-AM for 1 hour in the presence or absence of 1 μg/ml nocodazole, and wounded twice. Membrane disruption was indicated by the loss of calcein (Fig. 7A). When the cell membrane resealed, the fluorescent intensity stabilized (bars in Fig. 7A). To compare the timing of membrane resealing in each condition, the resealing rate was defined as the inverse of the resealing

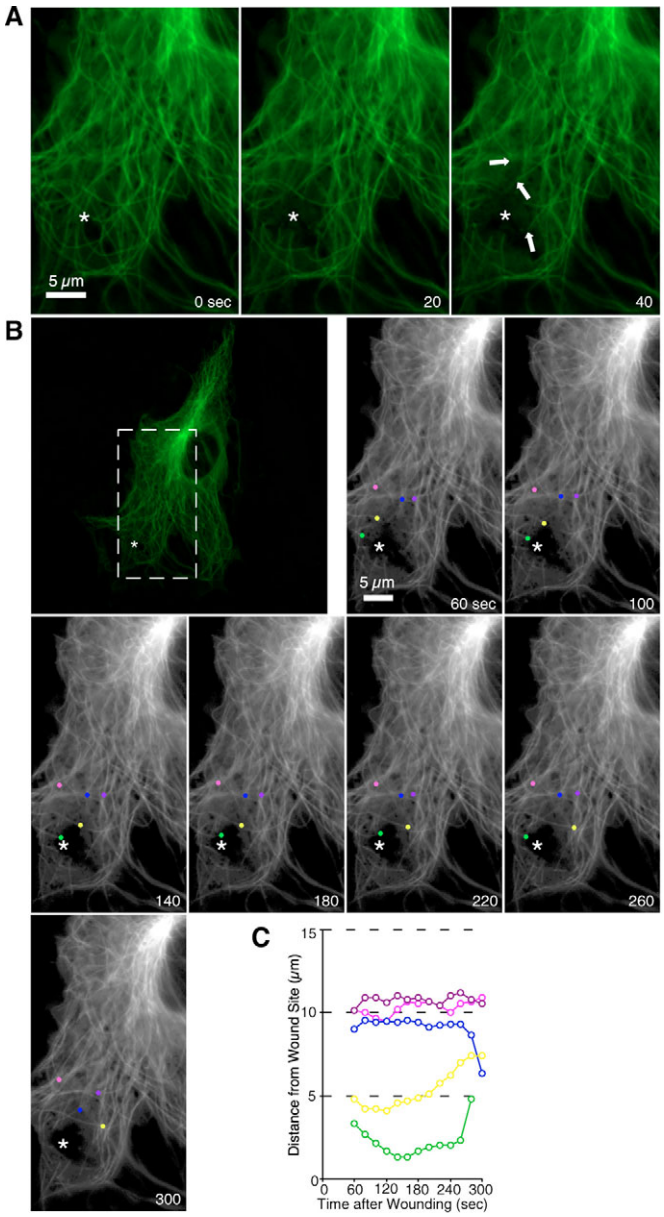

Fig. 3. Disassembly and reassembly of MTs upon cell membrane disruption is dependent on extracellular Ca^{2+} concentration. (A) A PtK2 cell expressing α-tubulin-EGFP was wounded in 0.4 mM-Ca^{2+} Ringer's solution. The asterisk indicates the site of cell membrane disruption. The cell membrane disruption induced MT disassembly around the wound site, but the propagation of the MT disassembled area was slower than in 1.8 mM Ca^{2+} Ringer's solution. Arrows indicate disassembled MTs. (B,C) MT ends did not approach the wound site in 0.4 mM Ca^{2+} Ringer's solution. Colored dots indicate selected MT ends.

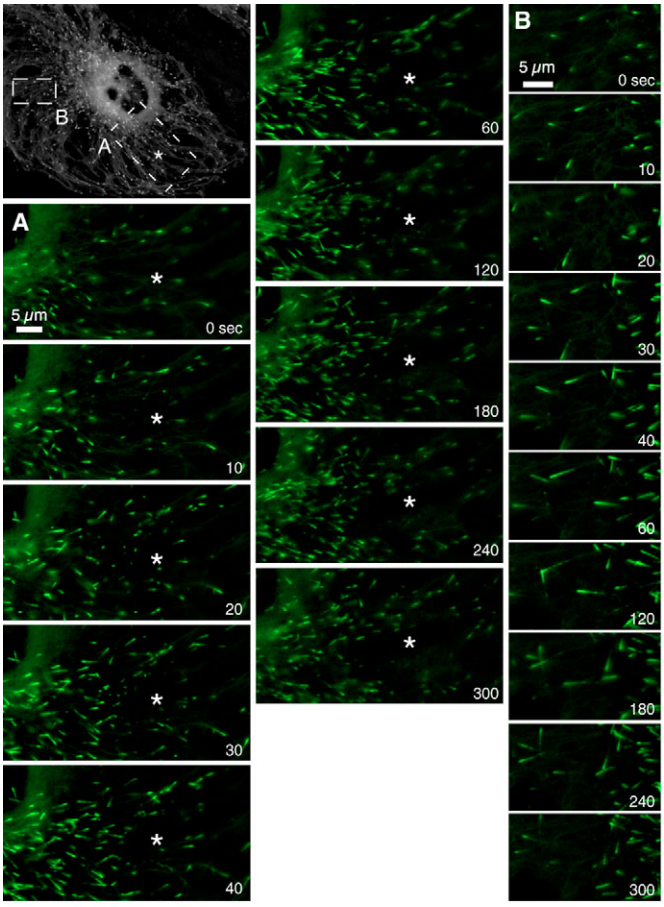

Fig. 4. Recruitment of EB1 to the MTs upon cell membrane disruption is dependent on Ca^{2+}. A PtK2 cell expressing EB1-GFP was wounded in 0.4 mM-Ca^{2+} Ringer's solution. The asterisk indicates the site of cell membrane disruption. A slight increase in the number of bright EB1-GFP comets was observed throughout the cell, however there was no obvious increase in the number of EB1-comets and directional movement of the comets around the wound site in this condition. A movie is available in supplementary material (Movie 3).

time in seconds. When cells were wounded in the absence of nocodazole, second membrane resealing was facilitated (Fig. 7) as shown in other cell types previously (Togo et al., 1999; Shen and Steinhardt, 2005). When cells treated with nocodazole were wounded, the initial resealing rate was not affected by this treatment. On the other hand, nocodazole prevented membrane resealing at the second wound. Eight out of 12 cells could not survive a second membrane disruption, whereas only two out of 13 cells could not survive a second membrane disruption in control experiments. These results support the idea that the vesicles required for the second membrane resealing are derived from the Golgi complex and/or the region of the TGN along MTs in a PKC-dependent manner.

Discussion

Plasma membrane disruption evokes a rapid exocytosis, which is essential for successful membrane resealing (McNeil and Steinhardt, 2003). It has previously been shown that the rate of membrane resealing with repeated wounds at the same site is facilitated, and that this response requires both Ca^{2+} and PKC activity, and is sensitive to BFA (Togo et al., 1999; Shen and Steinhardt, 2005). Lowering the temperature below 20°C also blocked facilitation, as expected from a block of Golgi function at that temperature (Togo et al., 1999). When FM1-43-loaded cells were wounded twice, exocytosis at the second wound, revealed by FM1-43 destaining, was less than at the initial wound (Togo et al., 1999). Therefore, these results suggest that the PKC-dependent short-term facilitation reflects the availability of a newly generated vesicle pool from the region of the TGN that is not labeled with FM1-43. Furthermore, same-site facilitation was found to be a polarized reaction only to the site where the calcium-sensitive vesicle pool had been depleted by a previous membrane disruption (Togo et al., 2003; Shen and Steinhardt, 2005). BFA did not affect the membrane resealing of an initial wound (Togo et al., 1999), even though several studies have shown that BFA also induces membrane tubulation of endosomes and lysosomes (Klausner et al., 1992). These results strongly suggest that the direction of vesicle transport from the region of the TGN to the plasma membrane is actively regulated upon cell membrane disruption.

The present study shows that membrane disruption triggers recruitment of EB1 to the MTs especially around the wound site and stimulates elongation of MTs toward the wound site.

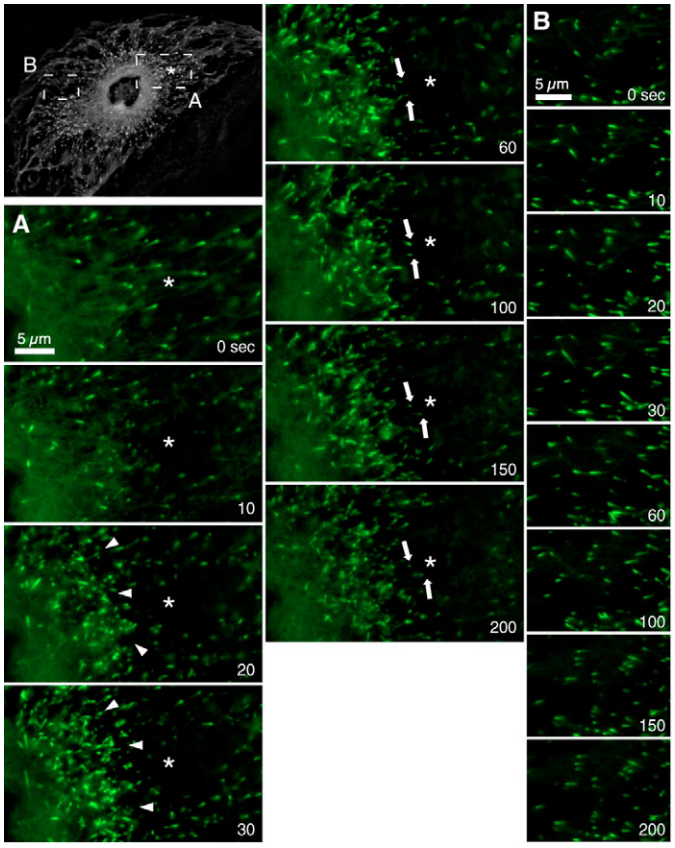

Fig. 5. Disassembly and reassembly of MTs upon cell membrane disruption are independent of PKC activity. A PtK2 cell expressing EB1-GFP was wounded in 1.8 mM Ca^{2+} Ringer's solution containing 1 μM Gö-6976. The asterisk indicates the site of cell membrane disruption. Numerous EB1-GFP comets appeared within 30 seconds of membrane disruption (arrowheads). Some comets approached the wound site (arrows). A movie is available in supplementary material (Movie 4). A slight increase in the number of bright EB1-GFP comets was also observed throughout the cell.

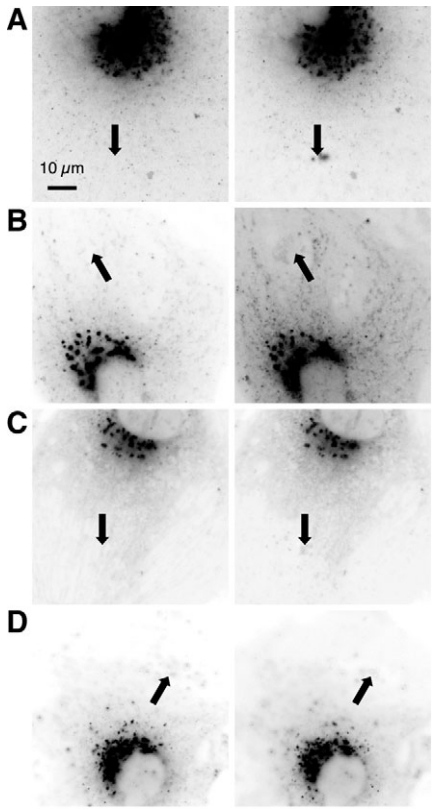

Fig. 6. Cell membrane disruption stimulates the delivery of NBD lipids toward the wound site along MTs in a PKC- and temperature-dependent manner. PtK2 cells were incubated with 5 μM NBD C_6-ceramide/BSA for 30 minutes at 4°C, washed, warmed to 37°C for 30 minutes and wounded with a glass needle. Arrows indicate the sites of cell membrane disruption. Left panel, before wounding; right panel, 5 minutes after wounding. (A) control; (B) 1 μM Gö-6976; (C) 1 μg/ml nocodazole; (D) 20°C. Images are inverted for easier visualization.

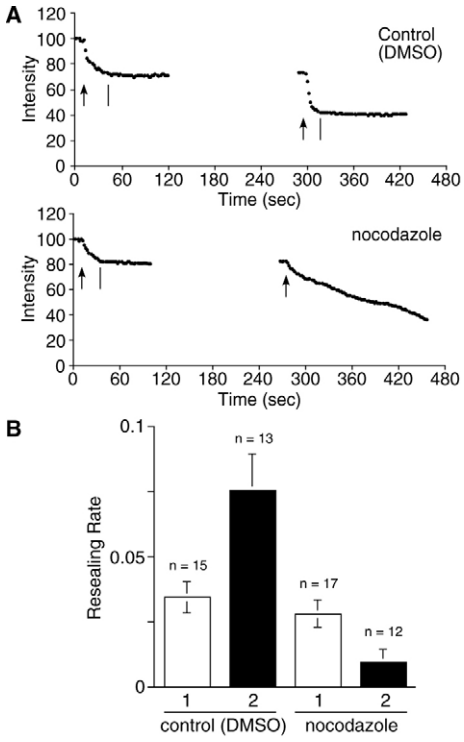

Fig. 7. Nocodazole treatment blocked membrane resealing at the second wound. (A) Cells were loaded with 1 μM calcein-AM for 1 hour in the presence or absence of 1 μg/ml nocodazole and wounded twice (arrows). Membrane disruption is indicated by the loss of calcein fluorescence. Bars mark the completion times of membrane resealing. Units of fluorescent intensity were normalized to 100% before the initial wounding. (B) Comparison of membrane resealing rates at the initial and second wounds. The resealing rates were defined as the inverse of the resealing time in seconds. For cells that failed to reseal, the rate was defined as zero. Values are the means ± s.e.m.

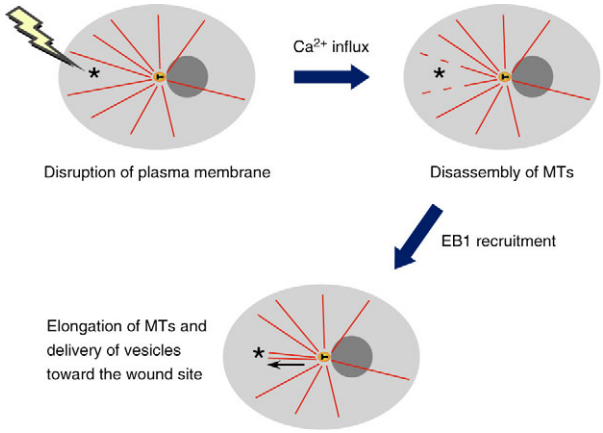

Fig. 8. Summary of MT rearrangement and membrane traffic toward the wound site. Ca^{2+} influx induced by cell membrane disruption initially stimulates MT disassembly around the wound site. Within 30 seconds of membrane disruption, EB1 is recruited to the MTs especially around the wound site, and stimulates elongation of MTs. Apparently vesicles are transported from the region of the TGN toward the wound site to refill the vesicle pool that was depleted by the initial wound.

This rearrangement of MTs seems to be required for the facilitated response of membrane resealing, because post-Golgi secretory traffic requires MTs (Toomre et al., 1999; Schmoranzer and Simon, 2003; Schmoranzer et al., 2003). In fact, membrane disruption stimulates the delivery of the fluorescent probe for Golgi-derived lipids, NBD C_6-ceramide, toward the wound site along MTs, as shown here by nocodazole inhibition. Furthermore, treatment of cells with nocodazole inhibited membrane resealing at the second wound, but not at the initial wound.

The present study suggests that Ca^{2+} influx upon cell membrane disruption locally regulates the affinity of EB1 for the MTs. PKCs have been associated with MTs in many cell types (Kiley and Parker, 1995; Garcia-Rocha et al., 1997; Hosotani et al., 2001; Kabir et al., 2001; Szalay et al., 2001; Nakhost et al., 2002), and, in yeast, *PKC1* regulates the function of MTs through *BIM1*, the yeast EB1 homologue (Hosotani et al., 2001). As shown in this study, however, PKC inhibition by Gö-6976 had no effect on the recruitment of EB1 upon cell membrane disruption. Further studies are required to clarify how Ca^{2+} influx upon cell membrane disruption stimulates EB1 recruitment to the MTs.

In contrast to the rearrangement of MTs, lipid traffic toward the wound site was PKC dependent. Gö-6976 does inhibit the facilitated response of membrane resealing for a second wound at the same site (Togo et al., 1999). Also, PKC activation by phorbol ester facilitates membrane resealing at the initial wound, but phorbol ester does not facilitate membrane resealing if cells are pretreated with BFA (Togo et al., 1999). These results support the hypothesis that PKC stimulates the regulated secretory pathway from the region of the TGN to the wound site, although the PKC subtypes involved in this process and substrates for PKC remain to be elucidated. These are currently under investigation. It should be noted that the delivery of fluorescent lipids toward the wound site was inhibited when cells were wounded at 20°C. This result further suggests that membrane traffic to the wound site from the region of the TGN was by a vesicle-mediated process, because incubation at low temperature blocks vesicle transport from the Golgi complex (Matlin and Simons, 1983; Saraste and Kuismanen, 1984). However, BFA and lower temperatures may have pleiotropic effects disrupting most endosomes and trafficking in addition to their dispersal and the ablation of Golgi function. An alternative mechanism would be mobilization of a store of vesicles that was previously stable and inactive and that therefore had not been labeled by the pretreatment with FM1-43 (Togo et al., 1999).

Wounding the cell membrane evokes a series of membrane-trafficking events at a distinct time and place ranging from the immediate Ca^{2+}-regulated exocytosis of docked vesicles to the generation, recruitment, and transport of new ones. Membrane disruption stimulates Ca^{2+}-dependent disassembly of MTs around the wound site, which is followed by elongation of MTs toward the wound site (Fig. 8). Membrane disruption also stimulates lipid traffic from the region of the TGN toward the wound site, possibly along elongated MTs. These responses may refill the vesicle pool around the wound site that is depleted by a previous membrane disruption. The adaptive response leading to faster cell membrane resealing at repeated

wounding would work to minimize the toxic effects of excessive Ca^{2+} entry (Trump and Berezesky, 1995) and the loss of crucial cellular constituents.

Materials and Methods

Cell culture

PtK2 cells were grown in minimum essential medium (MEM) supplemented with 100 IU/ml penicillin, 100 mg/ml streptomycin, 2 mM L-glutamine, 1× non-essential amino acids (all media components were from Invitrogen, Carlsbad, CA) and 10% fetal calf serum (Moregate Biotech, Bulimba, Australia) at 37°C in a 5% CO_2 humidified atmosphere. Cells for experiments were plated on glass-based 35 mm dishes (Asahi Techno Glass, Chiba, Japan).

Transfection

The expression vector for enhanced GFP (EGFP)-α-tubulin was purchased from Clontech Laboratories (Mountain View, CA). EB1-GFP plasmid DNA was kindly provided by Y. Mimori-Kiyosue (KAN Research Institute, Kyoto, Japan) (Mimori-Kiyosue et al., 2000). Vectors were transfected into cells using the CalPhos transfection kit (Clontech) in accordance with the manufacturer's protocol. Cells were observed 48 hours after the transfection.

Fluorescent lipid-labeling of cells

A complex of NBD C_6-ceramide with defatted BSA was purchased from Molecular Probes (Eugene, OR). Cultures were incubated with 5 μM NBD C_6-ceramide/BSA in Hanks' balanced salt solution (HBSS, Invitrogen) for 30 minutes at 4°C, washed several times with ice-cold HBSS, and further incubated in fresh HBSS for 30 minutes at 37°C.

Wounding and image analysis

During wounding experiments, the cells were maintained either in 1.8 mM or in 0.4 mM Ca^{2+} Ringer's solution. Ca^{2+}-free Ringer's solution contained 138 mM NaCl, 2.7 mM KCl, 1.06 mM $MgCl_2$, 5.6 mM D-glucose and 12.4 mM HEPES, pH 7.25. A stock solution of 100 mM $CaCl_2$ was used to adjust the concentration of Ca^{2+}.

The cells were observed on an IX-71 inverted microscope (Olympus, Tokyo, Japan) equipped with a PlanApo 60×/1.40 NA oil-immersion objective. Cells were kept at 37°C during observation unless otherwise stated, and were wounded with a glass needle using an Injectman 5179 and Transjector 5246 (Eppendorf, Hamburg, Germany). The time setting for wounding was 0.3 seconds. Images were collected with Retiga EXi Fast 1394 camera (QImaging, Burnaby, Canada) driven by SlideBook imaging software (Intelligent Imaging Innovations, Denver, CO). Exposure was controlled by a Lambda 10-2 optical filter changer (Sutter Instrument, Novato, CA) that was also driven by SlideBook. After collecting images, the cell was visually inspected and MTs were also observed for viability. If the cell membrane failed to reseal, MTs were completely disassembled throughout the cell owing to a continuous influx of Ca^{2+}. The data from these cells were discarded. If the cell survived the membrane disruption, then the cell was wounded again using bright field illumination, and the site of membrane disruption was recorded for later analysis. Images of EGFP-α-tubulin and EB1-GFP were then processed using the 'No Neighbors' deconvolution menu with SlideBook software to reduce out-of-focus haze and to enhance contrast. The stored frames were subsequently exported into TIFF format. The TIFF series was then converted into a QuickTime movie.

Estimation of the resealing rate

Calcein-AM (Molecular Probes) was loaded into the cells in the presence or absence of 1 μg/ml nocodazole for 1 hour at 37°C. Then the cells were wounded with a glass needle in 1.8 mM Ca^{2+} Ringer's solution as described above, and the fluorescence of calcein was monitored. A persistent decrease of fluorescent intensity (as an indicator of dye loss) indicates resealing failure. A transient decrease of fluorescent intensity indicates successful resealing. The resealing rate was defined as the inverse of resealing time in seconds. For cells that failed to reseal, the rate was defined as zero.

I thank Dr Y. Mimori-Kiyosue, KAN Research Institute, Kyoto, Japan, for generous gift of an EB1-GFP plasmid. I also thank Drs Richard A. Steinhardt and Janet M. Alderton for discussion and comments on this study. This study was supported by a Grant-in-Aid from the Ministry of Education, Culture, Sports, Science and Technology, Japan.

References

Bi, G.-Q., Alderton, J. M. and Steinhardt, R. A. (1995). Calcium-regulated exocytosis is required for cell membrane resealing. *J. Cell Biol.* **131**, 1747-1758.

Busch, K. E. and Brunner, D. (2004). The microtubule plus end-tracking proteins mal3p and tip1p cooperate for cell-end targeting of interphase microtubules. *Curr. Biol.* **14**, 548-559.

Garcia-Rocha, M., Avila, J. and Lozano, J. (1997). The ζ isozyme of protein kinase C binds to tubulin through the pseudosubstrate domain. *Exp. Cell Res.* **230**, 1-8.

Hosotani, T., Koyama, H., Uchino, M., Miyakawa, T. and Tsuchiya, E. (2001). *PKC1*, a protein kinase C homologue of *Saccharomyces cerevisiae*, participates in microtubule function through the yeast EB1 homologue, *BIM1*. *Genes Cells* **6**, 775-788.

Kabir, N., Schaefer, A. W., Nakhost, A., Sossin, W. S. and Forscher, P. (2001). Protein kinase C activation promotes microtubule advance in neuronal growth cones by increasing average microtubule growth lifetimes. *J. Cell Biol.* **152**, 1033-1043.

Kiley, S. C. and Parker, P. J. (1995). Differential localization of protein kinase C isozymes in U937 cells: evidence for distinct isozyme functions during monocyte differentiation. *J. Cell Sci.* **108**, 1003-1016.

Klausner, R. D., Donaldson, J. G. and Lippincott-Schwartz, J. (1992). Brefeldin A: insights into the control of membrane traffic and organelle structure. *J. Cell Biol.* **116**, 1071-1080.

Lipsky, N. G. and Pagano, R. E. (1985a). A vital stain for the Golgi apparatus. *Science* **228**, 745-747.

Lipsky, N. G. and Pagano, R. E. (1985b). Intracellular translocation of fluorescent sphingolipids in cultured fibroblasts: endogenously synthesized sphingomyelin and glucocerebroside analogues pass through the Golgi apparatus en route to the plasma membrane. *J. Cell Biol.* **100**, 27-34.

Ma, Y., Shakiryanova, D., Vardya, I. and Povov, S. V. (2004). Quantitative analysis of microtubule transport in growing nerve processes. *Curr. Biol.* **14**, 725-730.

Martiny-Baron, G., Kazanietz, M. G., Mischak, H., Blumberg, P. M., Kochs, G., Hug, H., Marmé, D. and Schächtele, C. (1993). Selective inhibition of protein kinase C isozymes by the indolocarbazole Gö 6976. *J. Biol. Chem.* **268**, 9194-9197.

Matlin, K. S. and Simons, K. (1983). Reduced temperature prevents transfer of a membrane glycoprotein to the cell surface but does not prevent terminal glycosylation. *Cell* **34**, 233-243.

McNeil, P. L. and Steinhardt, R. A. (2003). Plasma membrane disruption: repair, prevention, adaptation. *Annu. Rev. Cell Dev. Biol.* **19**, 697-731.

Mimori-Kiyosue, Y., Shiina, N. and Tsukita, S. (2000). The dynamic behavior of the APC-binding protein EB1 on the distal ends of microtubules. *Curr. Biol.* **10**, 865-868.

Nakhost, A., Kabir, N., Forscher, P. and Sossin, W. S. (2002). Protein kinase C isoforms are translocated to microtubules in neurons. *J. Biol. Chem.* **277**, 40633-40639.

O'Brien, E. T., Salmon, E. D. and Erickson, H. P. (1997). How calcium causes microtubule depolymerization. *Cell Motil. Cytoskeleton* **36**, 125-135.

Salaycik, K. J., Fagerstrom, C. J., Murthy, K., Tulu, U. S. and Wadsworth, P. (2005). Quantification of microtubule nucleation, growth and dynamics in wound-edge cells. *J. Cell Sci.* **118**, 4113-4122.

Saraste, J. and Kuismanen, E. (1984). Pre- and post-Golgi vacuoles operate in the transport of Semliki Forest virus membrane glycoproteins to the cell surface. *Cell* **38**, 535-549.

Schmoranzer, J. and Simon, S. M. (2003). Role of microtubules in fusion of post-Golgi vesicles to the plasma membrane. *Mol. Biol. Cell* **14**, 1558-1569.

Schmoranzer, J., Kreitzer, G. and Simon, S. M. (2003). Migrating fibroblasts perform polarized, microtubule-dependent exocytosis towards the leading edge. *J. Cell Sci.* **116**, 4513-4519.

Schuyler, S. C. and Pellman, D. (2001). Microtubule "plus-end-tracking proteins": the end is just the beginning. *Cell* **105**, 421-424.

Shen, S. S. and Steinhardt, R. A. (2005). The mechanisms of cell membrane resealing in rabbit corneal epithelial cells. *Curr. Eye Res.* **30**, 543-554.

Steinhardt, R. A., Bi, G.-Q. and Alderton, J. M. (1994). Cell membrane resealing by a vesicular mechanism similar to neurotransmitter release. *Science* **263**, 390-393.

Szalay, J., Bruno, P., Bhati, R., Adjodha, J., Schueler, D., Summerville, V. and Vazeos, R. (2001). Associations of PKC isoforms with the cytoskeleton of B16F10 melanoma cells. *J. Histochem. Cytochem.* **49**, 49-66.

Tirnauer, J. S. and Bierer, B. E. (2000). EB1 proteins regulate microtubule dynamics, cell polarity, and chromosome stability. *J. Cell Biol.* **149**, 761-766.

Tirnauer, J. S., Grego, S., Salmon, E. D. and Mitchison, T. J. (2002). EB1-microtubule interactions in *Xenopus* egg extracts: role of EB1 in microtubule stabilization and mechamisms of targeting to microtubules. *Mol. Biol. Cell* **13**, 3614-3626.

Togo, T., Alderton, J. M., Bi, G.-Q. and Steinhardt, R. A. (1999). The mechanism of facilitated cell membrane resealing. *J. Cell Sci.* **112**, 719-731.

Togo, T., Krasieva, T. B. and Steinhardt, R. A. (2000). A decrease in membrane tension precedes successful cell membrane repair. *Mol. Biol. Cell* **11**, 4339-4346.

Togo, T., Alderton, J. M. and Steinhardt, R. A. (2003). Long-term potentiation of exocytosis and cell membrane repair in fibroblasts. *Mol. Biol. Cell* **14**, 93-106.

Toomre, D., Keller, P., White, J., Olivo, J.-C. and Simons, K. (1999). Dual-color visualization of *trans*-Golgi network to plasma membrane traffic along microtubules in living cells. *J. Cell Sci.* **112**, 21-33.

Trump, B. F. and Berezesky, I. K. (1995). Calcium-mediated cell injury and cell death. *FASEB J.* **9**, 219-228.